Journal of the European Ceramic Society 22 (2002) 1897–1904

www.elsevier.com/locate/jeurceramsoc

Stability of intergranular phases in hot-pressed Si_3N_4 studied with mechanical spectroscopy and in-situ high-temperature XRD

R.G. Duan, G. Roebben, J. Vleugels, O. Van der Biest*

Department of Metallurgy and Materials Engineering, Katholieke Universiteit Leuven, Kasteelpark Arenberg 44, B-3001 Heverlee, Belgium

Received 10 January 2001; received in revised form 9 November 2001; accepted 17 November 2001

Abstract

The impulse excitation technique (IET) and high temperature X-ray diffraction (HTXRD) were used to investigate the intergranular glass phase and its crystallisation behaviour in four hot-pressed silicon nitrides. The internal friction or damping peak height measured with IET near the glass transition temperature, T_g, is used as a qualitative indicator for the amount of residual intergranular amorphous phase after sintering. Silicon nitride powder was hot-pressed with different sintering additives. The silicon nitride containing 4 wt.% Al_2O_3 does not reveal an internal friction peak at T_g, i.e. it does not contain a significant amount of intergranular glass phase. Three other silicon nitrides, containing either 8 wt.% Y_2O_3, 6 wt.% Y_2O_3+2 wt.% Al_2O_3, or 2 wt.% Y_2O_3+4 wt.% Al_2O_3+2 wt.% TiN, do show an internal friction peak near T_g. This "T_g-peak" is nearly unaffected by heating up to 1400 °C in the silicon nitride with $Y_2O_3+Al_2O_3+TiN$ sintering aids, whereas the amount of intergranular glass in the ceramics containing either $Y_2O_3+Al_2O_3$ or Y_2O_3 as a sintering aid is strongly reduced by subsequent heating. As observed from HTXRD, the onset temperature of crystallisation of the intergranular glass in the ceramic containing $Y_2O_3+Al_2O_3$ sintering aids is about 1100 °C, with the formation of Y–N-apatite ($Y_{20}N_4Si_{12}O_{48}$) and O-sialon ($Al_{0.04}Si_{1.96}N_{1.96}O_{1.04}$). The O-sialon phase in the yttria and alumina containing ceramics, formed either during sintering or during heat treatment, is not stable at elevated temperatures and dissolves in the intergranular glass phase between 1300 and 1400 °C. The O-sialon phase in the ceramic without Y_2O_3 sintering additive, however, is thermally stable. The presence of Ti^{4+} ions in the intergranular glass phase is suggested to inhibit its crystallisation, resulting in a stable high temperature damping behaviour. © 2002 Elsevier Science Ltd. All rights reserved.

Keywords: Damping; Grain boundaries; Hot-pressing; Internal friction; Si_3N_4; X-ray methods

1. Introduction

The ideal structural ceramic should be able to maintain a high fracture strength and high fracture toughness up to the temperature range of the intended application. In addition, for long-term high temperature applications, a good sub-critical crack growth and creep resistance is required. Si_3N_4 materials have been produced with remarkable thermo-mechanical and tribological properties.[1–4] Nevertheless, fracture toughness remains a concern for a variety of potential applications.[5]

Due to the high covalent bonding character of the Si_3N_4 crystal structure, the self-diffusion coefficients of nitrogen and silicon atoms are low.[6] Therefore, Si_3N_4 materials cannot be densified using the classical solid-state sintering technique.[3] Full density can only be obtained by liquid-phase sintering. The most commonly used sintering aids are Al_2O_3, MgO, AlN, SiO_2, Y_2O_3, and rare earth oxides,[7–11] which lead to the formation of an intergranular glass phase. The residual intergranular glass phase after sintering is responsible for the reported degradation in mechanical properties at temperatures above about 1000 °C, owing to its softening.[12] Intergranular glass phases with a tailored composition will have a beneficial effect on the high-temperature properties of Si_3N_4. Moreover, crystallisation of the intergranular glass phase can positively influence the high-temperature properties of Si_3N_4.[13–16] Therefore, further development of Si_3N_4-based ceramics needs detailed knowledge on intergranular glass phases and their crystallisation behaviour.

This paper investigates the effect of the use of single sintering aids (Y_2O_3 and Al_2O_3) or combined sintering

* Corresponding author. Fax: +32-16-321992.
E-mail address: omer.vanderbiest@mtm.kuleuven.ac.be (O. Van der Biest).

0955-2219/02/$ - see front matter © 2002 Elsevier Science Ltd. All rights reserved.
PII: S0955-2219(01)00511-8

aids ($Y_2O_3 + Al_2O_3$ and $Y_2O_3 + Al_2O_3 + TiN$) on the intergranular glass phase and its crystallisation. Especially the role of Ti^{4+} ions is discussed, since Ti^{4+} ions have a complex influence on silicate glass structure and crystallisation.[17,18] Two techniques have been used. The internal friction measured with the impulse excitation technique (IET) at elevated temperatures provides information on the presence and relative amount of amorphous phases. Complementary data were obtained with high temperature X-ray diffraction (HTXRD), providing information on the crystalline phases, both silicon nitride and the intergranular phases into which the intergranular glass potentially transforms.

2. Experimental procedure

2.1. Sample preparation

The starting powders used are a commercial Si_3N_4 powder (HCST grade LC12-SX, 97% α-Si_3N_4, sub-micron particle size, 1.8–2.1 wt.% oxygen), Y_2O_3 powder (Aldrich Chemical Company, Inc., USA, purity of 99.99%), Al_2O_3 powder (Baikowski grade SM8, 95% α, sub-micron particle size), and TiN powder (Ceramyg, France, sub-micron particle size). Powder mixtures were prepared by alumina ball-milling (Retsch B.V. Netherlands) in an alumina vessel for 4 h in isopropanol. The powder/milling ball/propanol weight ratio was 1/4/4. The nominal composition of the powder mixtures is listed in Table 1. The Al_2O_3 pick-up during ball milling was assessed by XRF (Philips, PW2400 X-ray Spectrometer, Netherlands) and found to be <0.6 wt.%. After evaporation of the propanol, the powder mixture was put in a graphite container, coated with boron nitride. The samples were cold pressed at 40 MPa and subsequently hot-pressed (W100/150-2200-50LAX, KCE Sondermaschinen, Germany) in vacuum (0.1 Pa) at 1650 °C for 1 h with a mechanical load of 30 MPa. The heating rate was 50 °C/min, the cooling rate 20 °C/min. After removal of the boron nitride, the hot-pressed disks were machined into samples suitable for IET, HTXRD, and scanning electron microscopy (SEM).

2.2. Basic microstructure and mechanical properties

The hot-pressed Si_3N_4 ceramics were polished, coated with carbon, and observed with a scanning electron microscope (SEM) (XL30 FEG, Philips). Backscattered electron images were recorded at an accelerating voltage of 20 kV.

The density, ρ, was measured in ethanol according to the Archimedes-method. The Vickers hardness, H_{V10}, was measured on a Zwick hardness tester with an indentation load of 10 kg. The fracture toughness, K_{IC}, was obtained by the Vickers indentation technique, based on the crack length measurement of the radial crack pattern produced by Vickers indentation. The K_{IC} values were calculated using the formula: $K_{IC} = 0.016(E/H_v)^{1/2}(P/(c^{3/2}))$, where E is the elastic modulus, H_v the hardness, P the indentation load, and c the radial crack length.[19] The density, Vickers hardness, and fracture toughness of the different ceramics are summarised in Table 2.

Table 1
Compositions of the starting powder mixtures (wt.%)

	SN–Y8	SN–Y6Al2	SN–Al4	SN–Y2Al4Ti2
Si_3N_4	92	92	96	92
Y_2O_3	8	6	0	2
Al_2O_3	0	2	4	4
TiN	0	0	0	2

2.3. Impulse excitation technique (IET)

The rectangular beam-like samples (nominal dimensions $30\times4\times2$ mm^3 or $40\times4.5\times2$ mm^3, thickness tolerance <0.01 mm) were suspended in the nodes of their first bending vibration mode, and measured in a graphite IET furnace (HTVP 1750-C, IMCE, Diepenbeek, Belgium) in a nitrogen atmosphere. The vibration signal, captured by a microphone was analysed with the resonance frequency and damping analyser (RFDA, IMCE, Diepenbeek, Belgium) as described elsewhere.[20] Before heating, the furnace is three times evacuated and filled with N_2 (L'air Liquide dry nitrogen with 10 ppm H_2O). The sample is subjected to two subsequent thermal cycles from 100 to 1400 °C with a heating and cooling rate of 2 °C/min. The E-modulus was calculated from the bending vibration frequency f_b according to the equation proposed in ASTM E 1876-99:[21] $E = 0.9465(m(f_b)^2/b)(L^3/t^3)T_1$, with m, L, b and t, the sample weight, length, width, and thickness, respectively. T_1 is a correction factor, depending on the Poisson's ratio ν and the thickness/length ratio. The internal friction is calculated as $Q^{-1} = k/(\pi f_r)$, where k is the exponential decay parameter of the amplitude of a given free vibration component f_r.[20]

Table 2
Mechanical properties and resonance frequencies of the different ceramic grades

Ceramic grade	f_b (Hz)	E (GPa)	ρ (g/cm^3)	H_{v10} (kg/mm^2)	K_{IC} (MPa/m$^{1/2}$)
SN–Y8	25024	296±7	3.19	1332±13	4.4±0.2
SN–Y6Al2	11465	296±12	3.23	1605±13	4.8±0.3
SN–Al4	25995	305±20	3.13	1618±18	2.6±0.1
SN–Y2Al4Ti2	11216	302±13	3.19	1641±18	5.0±0.1

2.4. High temperature X-ray diffraction (HTXRD)

High temperature X-ray diffraction (HTXRD) was performed on a θ–θ diffractometer (3003-TT, Seifert, Ahrensburg, Germany) using CuK_α radiation (40 kV, 30 mA), with a parabolic multilayer mirror for parallel beam optics which reduces susceptibility to thermally induced sample position change, and with a long 0.4° collimator in front of the scintillation detector for increased angular resolution.

Room temperature XRD tests were performed to determine the unit cell parameters of the hexagonal silicon nitride lattice. An angular accuracy of 0.01° was achieved by careful alignment of the diffractometer. The ω-arm, with attached source, is aligned using a fine, long slit as a sample. The θ-arm, carrying the detector, is aligned using a Si-reference powder sample (National Bureau of Standard, Standard Reference Materials 640a). The substitution level, z, of the β-$Si_{6-z}Al_zO_zN_{8-z}$ solid solution was calculated from the unit cell parameters (nm) according to $a = 0.7603 + 0.00296z$ and $c = 0.2907 + 0.00255z$.[22] XRD was also used to estimate the α-Si_3N_4 to β-Si_3N_4 or α-SiYAlON to β-SiAlON ratio in the hot-pressed ceramics. The intensities of the (101) and combined (210) and (120) diffraction peaks of the β-phase and the (102) and (210) peaks of the α-phase reveal the relative phase volume fractions through the following equation: $\alpha/\beta = [I_{\alpha(102)} + I_{\alpha(210)}]/[I_{\beta(101)} + I_{\beta(210)}]$.[23] This approach neglects the possible influence of texture, but can serve as a first guideline.

The high temperature tests were done in an X-Ray furnace (HDK2.4, Johanna Otto, Hechingen, Germany) with a Ta heating element, surrounding the sample. Tests were performed in vacuum ($<10^{-8}$ Pa) between room temperature and 1400 °C. Diffraction spectra were acquired at room temperature, 750, 1000, 1100, 1200, 1300 and 1400 °C, both during heating and cooling. The heating and cooling rate between two measuring temperatures was 30 °C/min. The data were acquired in the 2θ range from 15 to 80° (step width = 0.04°, measuring time = 1 s/step).

3. Results

3.1. Microstructural analysis

Scanning electron microscopy observations in combination with X-ray diffraction analysis enabled the identification of the constituent phases in the different hot-pressed ceramic grades. The backscattered electron micrographs are presented in Fig. 1, whereas the results of the room and high temperature diffraction analysis are summarised in Table 3. Additional information on the substitution level of the β-sialon matrix and the α/β-phase ratio is given in Table 4.

XRD analysis reveals that the SN-Al4 ceramic is mainly composed of β-sialon and, in addition, contains a smaller amount of O-sialon ($Al_{0.04}Si_{1.96}N_{1.96}O_{1.04}$) phase. The α-$Si_3N_4$ starting powder was completely converted into O- and β-sialon during hot pressing since no residual α-Si_3N_4 could be detected from the XRD data. The dispersed darker O-sialon phase can be clearly distinguished from the brighter β-sialon matrix on the SEM micrograph shown in Fig. 1a. The composition of the β-sialon phase is $Si_{5.8}Al_{0.2}O_{0.2}N_{7.8}$ as calculated from the diffraction data (see Table 4). No crystalline phase changes were observed upon heating to 1400 °C.

The hot-pressed SN-Y8 ceramic contains β-Si_3N_4, α-Si_3N_4 and Y–N-apatite ($Y_{20}N_4Si_{12}O_{48}$). The dark phases are α- and β-Si_3N_4 crystals, and the brighter phases are yttrium-containing intergranular crystals and glasses (Fig. 1b). The α/β ratio is 0.14, indicating an incomplete conversion of the Si_3N_4 starting powder. The measured (Al,O) substitution level of the β-phase is 0 (±0.08), as could be expected from the absence of Al_2O_3 additives. Nevertheless, a small amount (<0.6 wt.%) of Al was picked-up from the alumina container and milling balls, as determined by XRF-analysis. This observation confirms the correct alignment of the XRD-goniometer. The SN–Y8 ceramic is not fully dense. The black spots in Fig. 1b are pores. No additional crystalline phases were formed during thermal cycling up to 1400 °C.

The crystalline phases in the SN–Y6Al2 ceramic were identified as α- and β-sialon, with an α/β ratio of 0.35. The dark phases are α- and β-sialon grains, and the white intergranular phase on the micrograph (Fig. 1c) should be amorphous since no other crystalline phase was observed with XRD. The substitution level of the β-sialon phase of about 0.1 is lower than in the SN–Al4 and SN–Y2Al4Ti2 ceramics (see Table 4), as could be expected from the lower alumina content in the starting powder mixture. The HTXRD experiments on the SN–Y6Al2 ceramic revealed the formation of O-sialon and Y–N-apatite ($Y_{20}N_4Si_{12}O_{48}$) at elevated temperature (see Table 3). Both phases were still detected at 1300 °C, but were absent at 1400 °C.

The SN–Y2Al4Ti2 ceramic comprises β-sialon, α-sialon, O-sialon and TiN. The spherical white TiN and the black O-sialon grains can be clearly observed on the micrograph shown in Fig. 1d. The α/β ratio is 0.18 and the substitution level of the β-sialon phase ($z = 0.24$) is comparable to that of the SN–Al4 ceramic. The O-sialon phase in the SN–Y2AlTi2 ceramic was found to dissolve above 1300 °C.

3.2. Impulse excitation results

The Young's modulus, E, of the four silicon nitride grades at room temperature has been calculated from the resonant frequencies, which are also determined by the geometry of the samples. The results are listed in

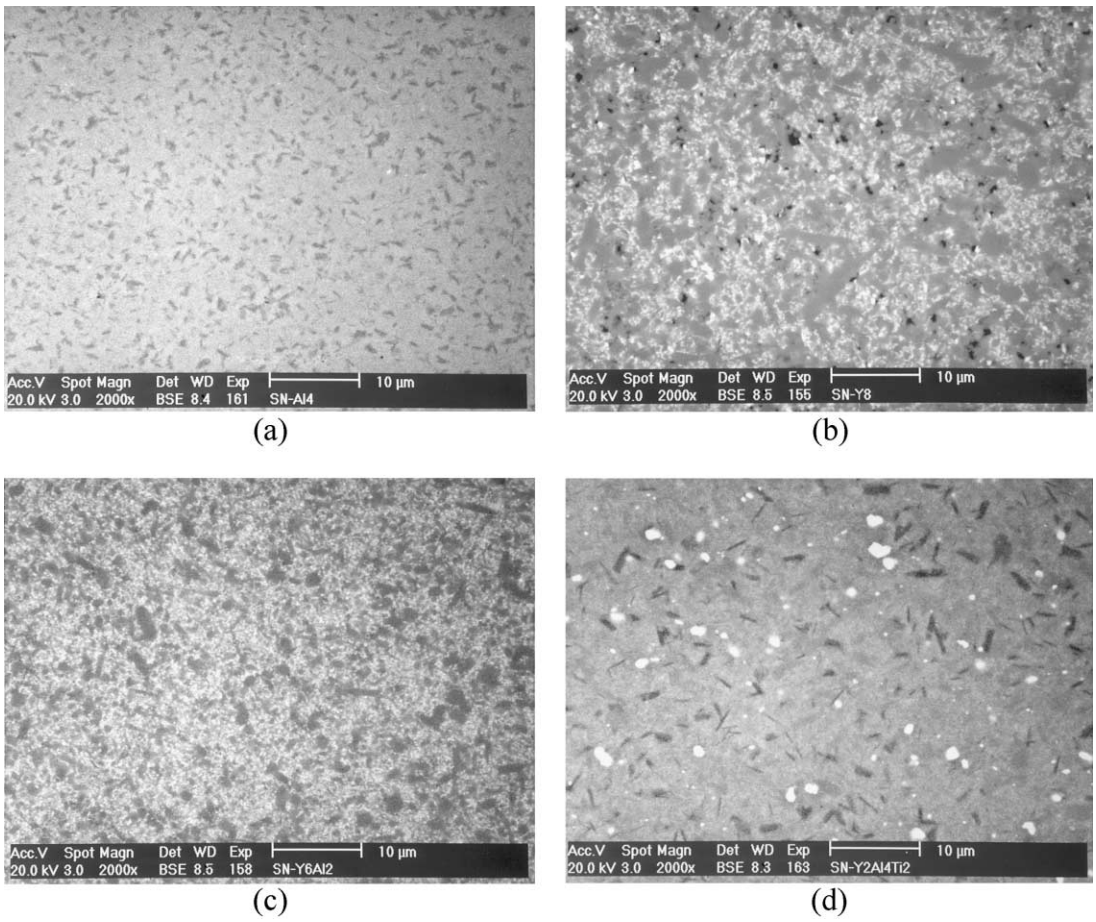

Fig. 1. Backscattered electron micrographs of the different ceramic grades. (a) SN–Al4, (b) SN–Y8, (c) SN–Y6Al2 and (d) SN–Y2Al4Ti2.

Table 3
Crystalline phase composition in the different ceramic grades, as obtained by HTXRD

Ceramic grade	Ceramic phases	20 °C	1000 °C	1100 °C	1200 °C	1300 °C	1400 °C
SN–Y8	α-Si_3N_4	+[a]	+	+	+	+	
	β-Si_3N_4	+	+	+	+	+	+
	$Y_{20}N_4Si_{12}O_{48}$	+	+	+	+	+	+
SN–Al4	β-sialon	+	+	+	+	+	+
	O-sialon	+	+	+	+	+	+
SN–Y6Al2	α-sialon	+	+	+	+	+	+
	β-sialon	+	+	+	+	+	+
	O-sialon	–[b]	–	+	+	+	–
	$Y_{20}N_4Si_{12}O_{48}$	–	–	+	+	+	–
SN–Y2Al4Ti2	α-sialon	+	+	+	+	+	+
	β-sialon	+	+	+	+	+	+
	O-sialon	+	+	+	+	+	–
	TiN	+	×	×	×	×	×

[a] +, phase present,
[b] –, phase absent.

Table 2. The internal friction data of the different ceramic grades during the first and second heating are presented in Figs. 2 and 3, respectively. Fig. 2 reveals a large internal friction peak in the SN–Y6Al2 and SN–Y2Al4Ti2 ceramics and a relatively small internal friction peak in the SN-Y8 sample. These peaks, which occur in the glass transition temperature (T_g) range of the intergranular silicate phases, are known to stem from relaxation in intergranular glass pockets.[24] As such, the location of the maximum internal friction provides a first estimate of T_g. The IET experiment did not reveal a T_g-peak for the SN–Al4 ceramics, indicating

Table 4
Lattice parameters and substitution level of the β-$Si_{6-z}Al_zO_zN_{8-z}$ phase and the α/β-phase ratio in the different ceramic grades

Ceramic grade	a (nm)	c (nm)	z (±0.08)	α/β
SN–Y6Al2	0.76048±0.00007	0.29098±0.00015	0.08	0.35
SN–Al4	0.76081±0.00020	0.29134±0.00026	0.21	0.00
SN–Y2Al4Ti2	0.76091±0.00030	0.29140±0.00027	0.24	0.18
SN–Y8	0.76030±0.00019	0.29073±0.00019	0.00	0.14

the absence or very low content of intergranular glass pockets in this sample. Moreover, the very low internal friction background indicates that the amorphous intergranular film between adjacent grains is absent. This can be concluded when comparing with the results of Pezzotti et al.[25] obtained on high purity Si_3N_4 and sialon materials. The T_g-peak of the SN–Y8, SN–Y6Al2, and SN–Y2Al4Ti2 ceramics is situated near 1070 °C. Considering the small difference in resonance frequencies of the tested samples (factor 2, Table 2), we neglect the frequency dependence of the T_g-peak position, and conclude that the T_g of the amorphous phase in the hot-pressed SN–Y8, SN–Y6Al2, and SN–Y2Al4Ti2 samples is comparable.

When the samples are measured throughout a second thermal cycle (Fig. 3), the internal friction peaks of the ceramics have changed to a different extent. The height of the internal friction peak of the SN–Y6Al2 and SN–Y8 ceramics decreased drastically, whereas the internal friction peak of the SN–Y2Al4Ti2 sample decreased by only 25%. The T_g of the residual intergranular glass phases of the SN–Y8, SN–Y6Al2, and SN–Y2Al4Ti2 samples in the second thermal cycle are 1020, 1000 and 1080 °C, respectively. The lower peak heights indicate that the amount of intergranular glass phase in samples SN–Y6Al2 and SN–Y8 has decreased after the first thermal cycle. The extent of this effect on the amorphous phase in the SN–Y2Al4Ti2 ceramic is less pronounced. The T_g shift in the consecutive thermal cycles is significant for the SN-Y8 and SN-Y6Al2 ceramics, whereas the T_g of the SN–Y2Al4Ti2 ceramic is hardly affected. This implies a significant composition change of the intergranular glass phase after thermal cycling for the SN–Y8 and SN–Y6Al2 ceramic, whereas the composition change in the SN–Y2Al4Ti2 ceramic is small. The addition of TiN to the silicon nitride appears to stabilise the intergranular glass phase.

3.3. Hardness and toughness

The SN–Y8 ceramic possesses a low hardness due to the incomplete densification. The hardness of the other ceramic grades is more comparable. The indentation fracture toughness is strongly related to the type and amount of sinter additives (Table 2). The SN–Al4 ceramic with no or only a very small amount of amorphous phase is very brittle. Of the four ceramics, the SN–Y2Al4Ti2 ceramic combines the higher hardness (1641 ± 18 kg/mm^2) and indentation fracture toughness (5.0 ± 0.1 MPa/m$^{1/2}$).

4. Discussion

4.1. The α-Si_3N_4 conversion during sintering

It is known that the sintering aids react with the SiO_2 that is present at the surface of the Si_3N_4 starting powder to form a liquid phase during sintering. Subsequently, the α-Si_3N_4 particles dissolve in this liquid phase, causing a local supersaturation and reprecipitation of β-Si_3N_4.[26,27] Different sintering aids will lead to the formation of different liquid phases with a composition-specific viscosity at 1650 °C. The lower the viscosity of the liquid phase, the faster the diffusion rate of Si^{4+} and N^{3-} ions and the higher the transformation rate from α- to β-Si_3N_4. In the process of transformation of Si_3N_4 from α- to β-structure, Al^{3+} and O^{2-} ions can enter the β-Si_3N_4 structure to replace some Si^{4+} and N^{3-} ions respectively, and form the β-sialon solid solution.

For the SN–Al4 ceramic, α-Si_3N_4 is completely converted to β-sialon during the hot-press cycle (1 h at 1650 °C), whereas α-Si_3N_4 is only partially converted to β-Si_3N_4 or β-sialon in the SN–Y8, SN–Y6Al2 and SN–Y2Al4Ti2 ceramics. Meanwhile, α-Si_3N_4 is converted to α-sialon in the SN–Y6Al2 and SN–Y2Al4Ti2 ceramics. The α to β-Si_3N_4 transformation rate is fastest for the SN–Al4 ceramic.

4.2. The influence of sintering aids on the type and stability of the intergranular glass phases

Upon cooling, the liquid phases formed during sintering devitrify partially or totally. The remainder solidifies as an intergranular glass phase. For oxynitride glasses, the basic structural units are $[SiN_xO_{4-x}]$ tetrahedra, where x equals to 0, 1, 2, 3, or 4.[28–30] Depending on the type and amount of sintering aids, other structural units emerge. Since the amount of alumina picked-up during milling is very low, the intergranular glass phase formed in the SN-Y8 ceramic is considered to be an Y–Si–O–N glass. In the Y–Si–O–N glass, the structural $[SiN_xO_{4-x}]$ units are linked by sharing nitrogen or oxygen atoms. Since Y_2O_3 is a network modifier, all Y^{3+} ions are located in the network holes, between the tetrahedron-chains.

Al_2O_3 is a network intermediate, i.e. it can be both network modifier and network former. In R_2O–Al_2O_3–SiO_2 glass, all Al^{3+} ions exist as network formers provided that $Al_2O_3/R_2O < 1$.[31,32] In the SN–Y6Al2 cera-

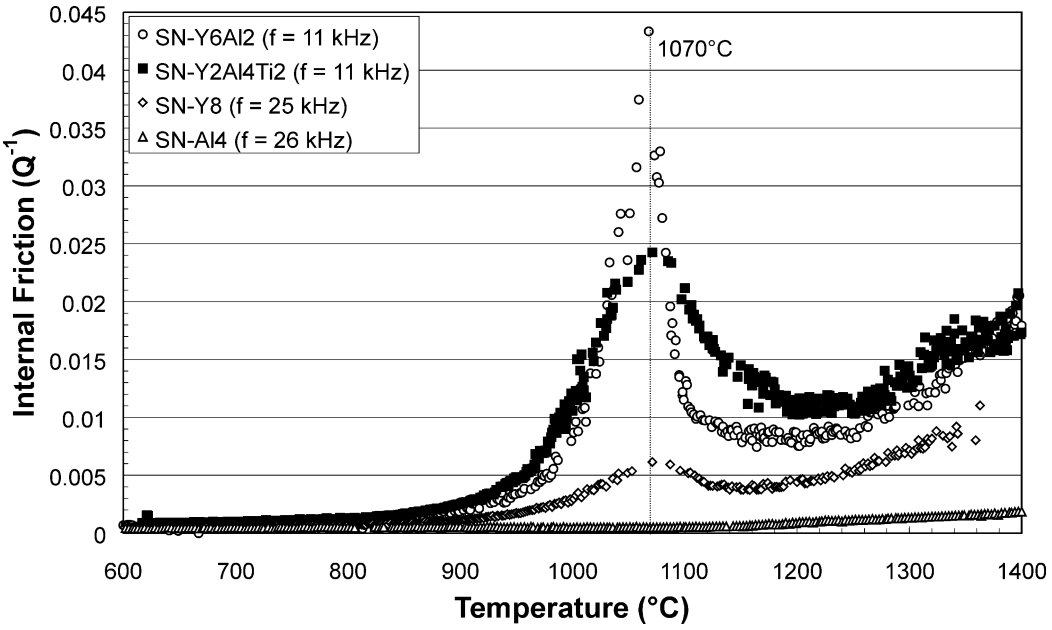

Fig. 2. Internal friction curves of the different ceramic grades during the first thermal cycle.

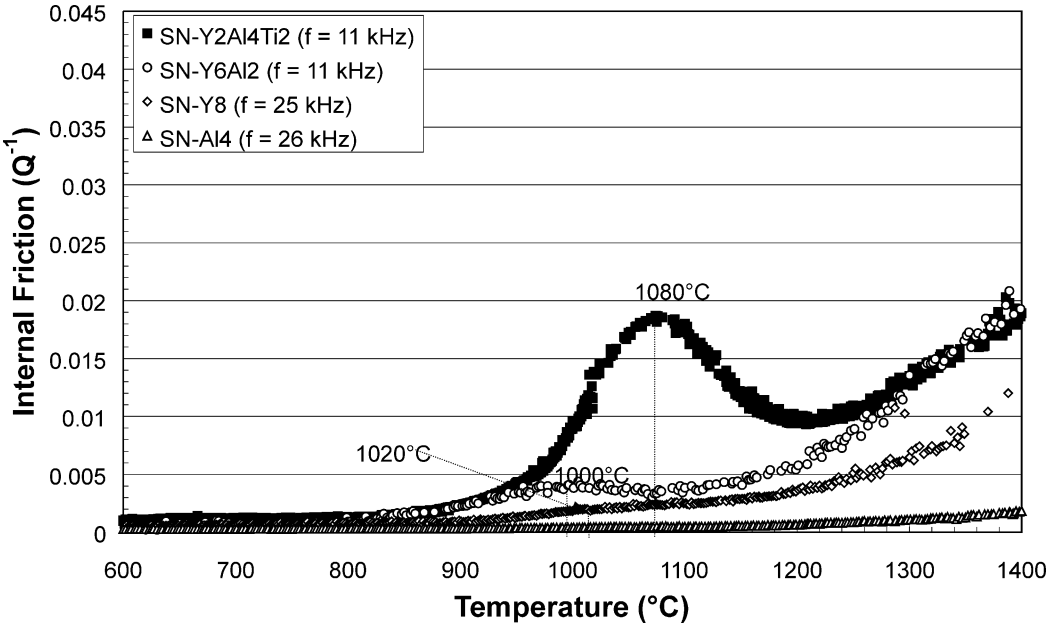

Fig. 3. Internal friction curves of the different ceramic grades during the second thermal cycle.

mic in this investigation, some Al^{3+} ions enter the α and β-sialon structure. The remaining fraction of Al^{3+} ions will enter the Y–Al–Si–O–N glass network structure as $[AlN_xO_{4-x}]$, where x is 1, 2, 3, or 4. These Al^{3+} ions will behave as a network former, because there is a large amount of Y^{3+} network modifiers in the liquid phase formed at 1650 °C in this composition. Due to the presence of network forming Al^{3+} ions in the liquid phase, the glass-forming ability of the liquid phase in the SN–Y6Al2 sample is larger than that in the SN–Y8 sample.

Because the internal friction peak of the intergranular glass phase in the SN–Y2Al4Ti2 ceramic after thermal cycling is different from those in the samples without TiN (Figs. 2 and 3), Ti^{4+} ions can be assumed to be present in the intergranular glass phase. This implies that the intergranular glass phase should be an Y–Al–Ti–Si–O–N glass. TiN powders always have a thin layer of TiO_2 on the surface, due to oxidation. This TiO_2 can indeed enter the intergranular glass phase as units of $[TiO_4]$.[17,33] Moreover, Ti^{4+} ions can substitute for Si

and Al in the $[SiN_xO_{4-x}]$ and $[AlN_xO_{4-x}]$ tetrahedra. Upon cooling, Ti^{4+} ions enter the glass network as $[TiN_xO_{4-x}]$, as this is a more stable unit than $[AlN_xO_{4-x}](x=0,1,2)$.[33] On the other hand, in the liquid phase formed at 1650 °C in the SN–Y2Al4Ti2 sample, the Y^{3+} ion content is lower than in SN–Y8 and SN–Y6Al2 ceramics. Therefore, some Al^{3+} ions exist as network modifiers in the intergranular glass phase in this ceramic. Because of the additional $[TiN_xO_{4-x}]$ units, the glass-forming ability of the liquid phase in the SN–Y2Al4Ti2 sample is higher than that in the SN–Y8 and SN–Y6Al2 ceramics.

Finally, the liquid phase in the SN–Al4 sample forms O-sialon ($Al_{0.04}Si_{1.96}N_{1.96}O_{1.04}$) during cooling. There is no or only a very low amount of residual intergranular glass phase in this ceramic, as shown by the absence of an internal friction peak in the IET experiments (see Figs. 2 and 3).

The stability, i.e. the resistance to crystallisation, of the amorphous phases is strongly influenced by the glass network structure. The presence of unstable $[AlN_xO_{4-x}]$ structure units renders the Y–Al–Si–O–N intergranular glass phase rather unstable. The additional $[TiN_xO_{4-x}]$ units in the Y–Al–Ti–Si–O–N glass stabilise this glass and hinder its crystallisation. After the heat treatment, the residual intergranular glass phase content in the SN–Y8 and SN–Y6Al2 ceramics, is strongly reduced as revealed by IET (see Figs. 2 and 3), whereas the glass content in the SN–Y2Al4Ti2 ceramic remained high. The IET observations are in agreement with the glass stability predictions. The main reason for the glass phase stability in the SN–Y2Al4Ti2 sample is the dissolution of Ti^{4+} ions into the glass network as a network former. The stability of the intergranular glass phase in the ceramic grades can be ranked as: SN–Y2Al4Ti2 > SN–Y8 > SN–Y6Al2.

The Y–Si–O–N glass in SN–Y8, the Y–Al–Si–O–N glass in SN–Y6Al2 and the Y–Al–Ti–Si–O–N glass in SN–Y2Al4Ti2 contain nitrogen. It has been pointed out that the higher the N^{3-} ion content in oxynitride glass, the higher the T_g.[34] This observation can be related to the change in glass transition temperature (T_g) of the intergranular glass phases in the present work. After heat treatment, the T_g of the Y–Si–O–N and Y–Al–Si–O–N glasses decreased from 1070 to 1020 °C and from 1070 to 1000 °C respectively. The T_g of the Y–Al–Ti–Si–O–N glass however slightly increased from 1070 to 1080 °C. A decrease of the nitrogen content in the Y–Al–Si–O–N glass in the SN–Y6Al2 ceramic can indeed be expected from the crystallisation of N-rich O-sialon (Table 3). The measured shift in the T_g temperature in the Y–Al–Ti–Si–O–N glass of the SN–Y2Al4Ti2 sample is very small, but could indicate that the nitrogen content has slightly increased. Again, this can be explained by the observed dissolution of the O-sialon phase at 1400 °C in the first heat treatment.

4.3. The O-sialon phase

The O-sialon phase ($Al_{0.04}Si_{1.96}N_{1.96}O_{1.04}$) is actually Si_2N_2O in which Si^{4+} and N^{3-} are partially substituted by Al^{3+} and O^{2-}.[35] Pure Si_2N_2O is difficult to obtain by classical sintering.[36] In this paper, a crystalline O-sialon phase is produced from the liquid phase in the SN–Al4 and SN–Y2Al4Ti2 samples during cooling, whereas it is formed in the SN–Y6Al2 ceramic when heat treated above 1100 °C.

The liquid phase in the SN–Al4 ceramic at 1650 °C is an Al–Si–O–N solution. For Al–Si–O–N glass, most Al^{3+} ions exist as network modifiers rather than as network formers. The resulting less stable glass structure facilitates the formation of the O-sialon during cooling of the liquid phase after sintering.

The liquid phase in the SN–Y2Al4Ti2 sample has an Y–Al–Ti–Si–O–N composition. When this liquid is cooled, some of the Al^{3+} ions will become network modifiers because of the low yttrium network modifier content and the more stable network structural unit $[TiN_xO_{4-x}]$ present. Again, the presence of some Al^{3+} ions as network modifiers enables the formation of O-sialon.

The intergranular glass phase in the SN–Y6Al2 ceramic is an Y–Al–Si–O–N glass, in which most of the Al^{3+} ions exist as network formers, because of the high Y^{3+} content. This inhibits the formation of O-sialon during liquid cooling. When the sample is heat treated at 1100 °C however, the $[AlN_xO_{4-x}]$ glass network structural units are not stable, as can be calculated from the formula in ref. 33. Some Al^{3+} ions change from network formers to network modifiers, and this slowly enhances the formation of O-sialon.

The process of the O-sialon phase formation is different in all three ceramic grades. The O-sialon phase is unstable at high temperatures. When heated at 1400 °C, the O-sialon phase in the SN–Y6Al2 and SN–Y2Al4Ti2 ceramic dissolves in the intergranular glass phase. The O-sialon phase in the SN–Al4 ceramic however is thermally stable, possibly due to the absence of an amorphous intergranular phase.

5. Conclusions

(1) IET, providing access to internal friction, was shown to be a valuable tool in the comparison and comprehension of Si_3N_4-grades with different intergranular phases. (2) Using only Al_2O_3 as a sintering aid improves the transformation of Si_3N_4 from α- to β-structure. (3) The intergranular glass phase formed in Si_3N_4 ceramics with $Y_2O_3 + Al_2O_3$ sintering aids is not stable. When heated to about 1100 °C, the intergranular glass phase starts to crystallise with the formation of Y–N-apatite ($Y_{20}N_4Si_{12}O_{48}$) and O-sialon ($Al_{0.04}Si_{1.96}$

$N_{1\cdot96}O_{1\cdot04}$). At 1400 °C, in the presence of intergranular Y–Al–Si–O–N and Y–Al–Ti–Si–O–N glass phases, the O-sialon crystals formed during sintering or heat treatment, are not stable. (4) The addition of TiN causes a stable high temperature damping behaviour. It is explained how the presence of $[TiN_xO_{4-x}]$ structural units makes the intergranular glass phase more stable. (5) A decrease/increase of the amount of N^{3-} ions in the intergranular glass phase is shown to increase/decrease the temperature at which an internal friction peak (i.e. the T_g peak) is observed.

Acknowledgements

R.G.Duan and G.R. thank the Fund for Scientific Research—Vlaanderen (FWO) for their research fellowships.

References

1. Jack, K. H., Review: sialons and related nitrogen ceramics. *J. Mater. Sci.*, 1976, **11**, 1135–1158.
2. Lange, F. F., Fabrication and properties of dense polyphase silicon nitride. *Am. Ceram. Soc. Bull.*, 1983, **62**, 1369–1374.
3. Ziegler, G., Heinrich, J. and Wotting, G., Review: relationship between processing, microstructure and properties of dense and reaction-bonded silicon nitride. *J. Mater. Sci.*, 1987, **22**, 3041–3086.
4. Kleebe, H.-J., Structure and chemistry of interfaces in Si_3N_4 ceramics studied by transmission electron microscopy. *J. Ceram. Soc. Japan*, 1997, **105**, 453–475.
5. Hirosaki, N., Akimune, Y. and Mitomo, M., Effect of grain growth of β-silicon nitride on strength, Weibull modulus, and fracture toughness. *J. Am. Ceram. Soc.*, 1993, **76**, 1892–1894.
6. Kijima, K. and Shirasaki, S., Nitrogen self-diffusion in silicon nitride. *J. Chem. Phys.*, 1976, **65**, 2668–2671.
7. Vleugels, J. and Van der Biest, O., Development, characterisation and oxidation behaviour of Si_3N_4–Al_2O_3 ceramics. *J. Eur. Ceram. Soc.*, 1994, **13**, 529–544.
8. Roebben, G., Donzel, L., Stemmer, S., Steen, M., Schaller, R. and Van der Biest, O., Viscous energy dissipation at high temperature in silicon nitride. *Acta Mater.*, 1998, **46**, 4711–4723.
9. Stemmer, S., Roebben, G. and Van der Biest, O., Evolution of grain boundary films in liquid phase sintered silicon nitride during high temperature testing. *Acta Mater.*, 1998, **46**, 5599–5606.
10. Trice, R. W. and Halloran, J. W., Mode 1 fracture toughness of a small-grained silicon nitride: orientation, temperature, and crack length effects. *J. Am. Ceram. Soc.*, 1999, **82**, 2633–2640.
11. Choi, H.-J., Lee, J.-G. and Kim, Y.-W., Oxidation behaviour of hot-pressed Si_3N_4 with Re_2O_3 (Re = Y, Yb, Er, La). *J. Euro. Ceram. Soc.*, 1999, **19**, 2757–2762.
12. Hoffmann, M. J., High-temperature properties of Si_3N_4 ceramics. *MRS Bulletin*, 1995, **2**, 28–32.
13. Sanders, W. A. and Mieskowski, D. M., Strength and microstructure of sintered Si_3N_4 with rare-earth-oxide additions. *J. Am. Ceram. Soc.*, 1985, **64**, 304–309.
14. Pierce, L. A., Mieskowski, D. M. and Sanders, W. A., Effect of grain-boundary crystallisation on the high temperature strength of silicon nitride. *J. Mater. Sci.*, 1986, **21**, 1345–1348.
15. Cinibulk, M. K., Thomas, G. and Johnson, S. M., Grain-boundary phase crystallisation and strength of silicon nitride sintered with a YSiAlON glass. *J. Am. Ceram. Soc.*, 1990, **73**, 1606–1612.
16. Tsuge, A., Nishida, K. and Komatsu, M., Effect of crystallising the grain-boundary glass phase on the high-temperature strength of hot-pressed Si_3N_4 containing Y_2O_3. *J. Am. Ceram. Soc.*, 1975, **58**, 323–326.
17. Duan, R. G., Liang, K. M. and Gu, S. R., The effect of Ti^{4+} on the site of Al^{3+} in the structure of CaO–Al_2O_3–SiO_2–TiO_2 system glass. *Mater. Sci. Engin. A*, 1998, **249**, 217–222.
18. Duan, R. G., Liang, K. M. and Gu, S. R., Effect of changing TiO_2 content on structure and crystallisation of CaO–Al_2O_3–SiO_2 system glasses. *J. Eur. Ceram. Soc.*, 1998, **18**, 1729–1735.
19. Anstis, G. R., Chantikul, P., Lawn, B. R. and Marshall, D. B., A critical evaluation of indentation techniques for measuring fracture toughness: 1, direct crack measurements. *J. Am. Ceram. Soc.*, 1981, **64**, 533–538.
20. Roebben, G., Bollen, B., Brebels, A., Van Humbeeck, J. and Van der Biest, O., Impulse excitation apparatus to measure resonant frequencies, elastic moduli, and internal friction at room and high temperature. *Rev. Sci. Instrum.*, 1997, **68**, 4511–4515.
21. ASTM E 1876-99, Am. Soc. Testing and Materials, 2000.
22. Ekstrom, T., Kall, P. O., Nygren, M. and Olsson, P. O., Dense single-phase β-sialon ceramics by glass-encapsulated hot isostatic pressing. *J. Mater. Sci.*, 1989, **24**, 1853–1861.
23. Grand, G., Demit, J., Ruste, J. and Torre, J. P., Composition and stability of Y–Si–Al–O–N solid solutions based on α-Si_3N_4 structure. *J. Mater. Sci. Lett.*, 1979, **14**, 1749–1751.
24. Donzel, L., Lakki, A. and Schaller, R., Glass transition and α relaxation in Y–Si–Al–O–N glasses and in Si_3N_4 ceramics studied by mechanical spectroscopy. *Philosophical Magazine A*, 1997, **76**, 933–944.
25. Pezzotti, G., Kleebe, H.-J., Okamoto, K. and Ota, K., Structure and viscosity of grain boundary in high-purity sialon ceramics. *J. Am. Ceram. Soc.*, 2000, **83**, 2549–2555.
26. Lifshitz, I. M. and Slyozov, V. V., The kinetics of precipitation from supersaturated solid solutions. *J. Phys. Chem. Solids*, 1961, **19**, 35–46.
27. Vetrano, J. S., Kleebe, H.-J., Hampp, E., Hoffmann, M. J. and Cannon, R. M., Epitaxial deposition of silicon nitride during post-sintering heat treatment. *J. Mater. Sci. Letters*, 1992, **11**, 1249–1252.
28. Tsukuma, K. and Akiyama, T., High temperature viscosity of nitrogen modified silica glass. *J. Non-Cryst. Solids*, 2000, **265**, 199–209.
29. Sato, R. K., Bolvin, J. and McMillan, P. F., Synthesis and characterisation of a SiAlON glass. *J. Am. Ceram. Soc.*, 1990, **73**, 2494–2497.
30. Kohn, S., Hoffbauer, W., Jansen, M., Franke, R. and Bender, S., Evidence for the formation of SiON glasses. *J. Non-cryst. Solids*, 1998, **224**, 232–243.
31. Day, D. E. and Rindone, G. E., Properties of soda aluminosilicate glasses, 1: refractive index, density, molar refractivity, and infrared absorption spectra. *J. Am. Ceram. Soc.*, 1962, **45**, 489–496.
32. Riebling, E. F., Structure of sodium aluminosilicate melts containing at least 50 mol.% SiO_2 at 1500 °C. *J. Chem. Phys.*, 1966, **44**, 2857–2865.
33. Duan, R. G., Liang, K. M. and Gu, S. R., The stable energy of glass structure unit. *Mater. Trans., JIM*, 1998, **39**, 1162–1163.
34. Hampshire, S., Flynn, R., Morrissey, V., Pomeroy, M., Rouxel, T., Besson, J.-L. and Goursat, P., Effects of temperature on viscosities and elastic modulus of oxynitride glass. *Key Eng. Mater.*, 1994, **89-91**, 351–356.
35. Trigg, M. B. and Jack, K. H., Solubility of aluminium in silicon oxynitride. *J. Mater. Sci. Lett.*, 1987, **6**, 407–408.
36. Bergman, B. and Heping, H., The influence of different oxides on the formation of Si_2N_2O from SiO_2 and Si_3N_4. *J. Eur. Ceram. Soc.*, 1990, **6**, 3–8.